Journal of the Mechanics and Physics of Solids 115 (2018) 230–247

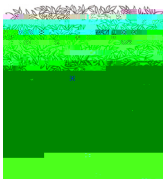

Table 1
Meaning and dimensions of mathematical symbols used in the manuscript.

Symbol	Meaning	Unit
b	Length of a chain's segment	m
C	Total chain density	mol/m^3
c, c_d	Density of the attached chains, density of the detached chains	mol/m^3
$\mathcal{D}$	The energy dissipation of chains	J/s
f	Probability density function of the end-to-end distance of chains	$1/m^3$
k_a	Association rate of active chains that are detached	1/s
k_d	Dissociation rate of active chains that are attached	1/s
k_B	Boltzmann constant	
$\mathcal{L}$, $\mathcal{L}^{-1}$	Langevin function and its inverse	
N	Number of segments in a polymer chain	
p	Lagrange multiplier that enforces incompressibility	Pa
$\mathbf{r}$	End-to-end vector of a chain	m
r	End-to-end	

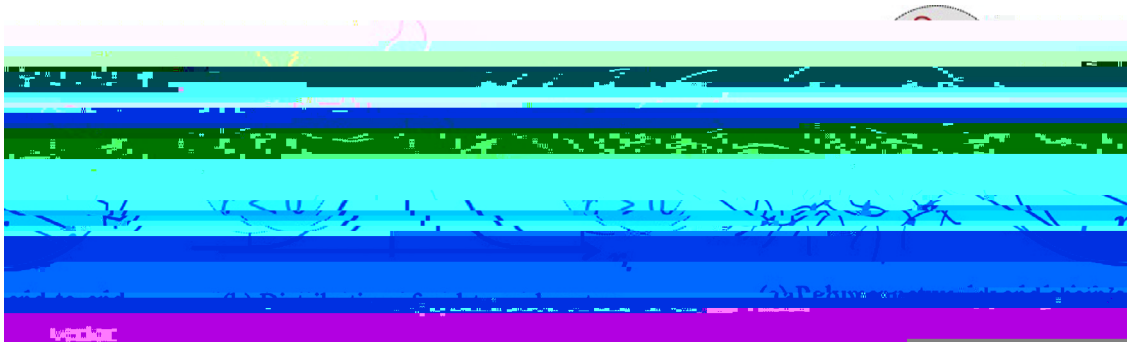

Fig. 1. (a) Cross-linked polymer network and

show that, when force free, the average end-to-end distance of a single chain is related to the number N and length b of Kuhn segments by $r_0 = \sqrt{N}b$. Further assuming that at a length-scale that is much larger than individual chains, the network is random and isotropic, the stress-free chain distribution can be expressed as a normal distribution f_0 with a zero mean and a standard deviation $\sqrt{N}b/3$ in each of the three spatial directions. We write (Treloar, 1975):

$$f_0(\boldsymbol{\lambda}) = \left(\frac{3}{2\pi N b^2}\right)^{\frac{3}{2}} \exp\left[-3\boldsymbol{\lambda}\right]$$

condition $\varphi(\boldsymbol{\lambda}, 0)$ and boundary conditions $\varphi \to 0$ as $\boldsymbol{\lambda} \to \infty$. Under the assumption that individual chains

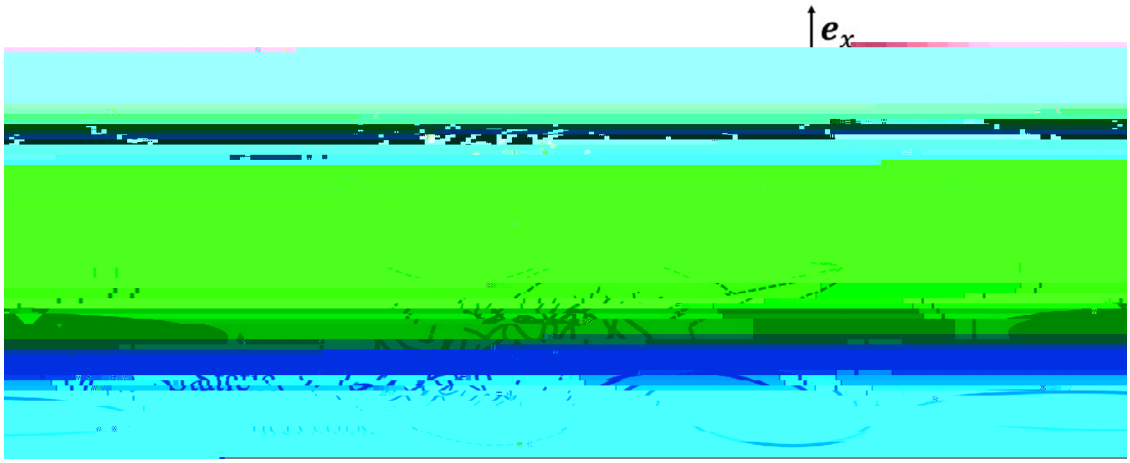

Fig. 4. Schematic of the problem set-up. We consider a polymer made of a static network with active chain concentration c^s and a dynamic network with active total concentration c^d. The response of this polymer is assessed with an unconfined uniaxial compression (or tensile) test, under different rates of loading and unloading histories.

where the superscript i is used to designate each network ($i = s, d$). A version of the kinetic equations in this context are presented next for each network and the entire polymer.

Static network. In the static network, the concentration remains constant over time $c^s(t) = c^s$ and the components of the distribution tensor can be determined from the fact that $\boldsymbol{\mu}^s = J\boldsymbol{F}^T\boldsymbol{F} = diag(\lambda^2, 1/\lambda, 1/\lambda)$ (using the incompressibility condition). This yields:

$$\mu^s = \lambda^2 \quad \text{and} \quad \mu^s_* = 1/\lambda. \tag{31}$$

Dynamic network. In the dynamic network, the evolution of concentrations and distribution tensors are determined from Eqs.

Table 2
Material parameters for a permanent/dynamic double network with nonlinear chain elasticity.

Type	Symbol	Meaning	Unit
Dimensional	C	Total chain concentration	mole/volume
	k_d	Detachment rate	1/time
Non-dimensional	N	Chain length	no unit
	$k_a^* = k_a/k_d$	Attachment rate	no unit
	$\alpha = c^s/c^t$	Permanent chain fraction	no unit

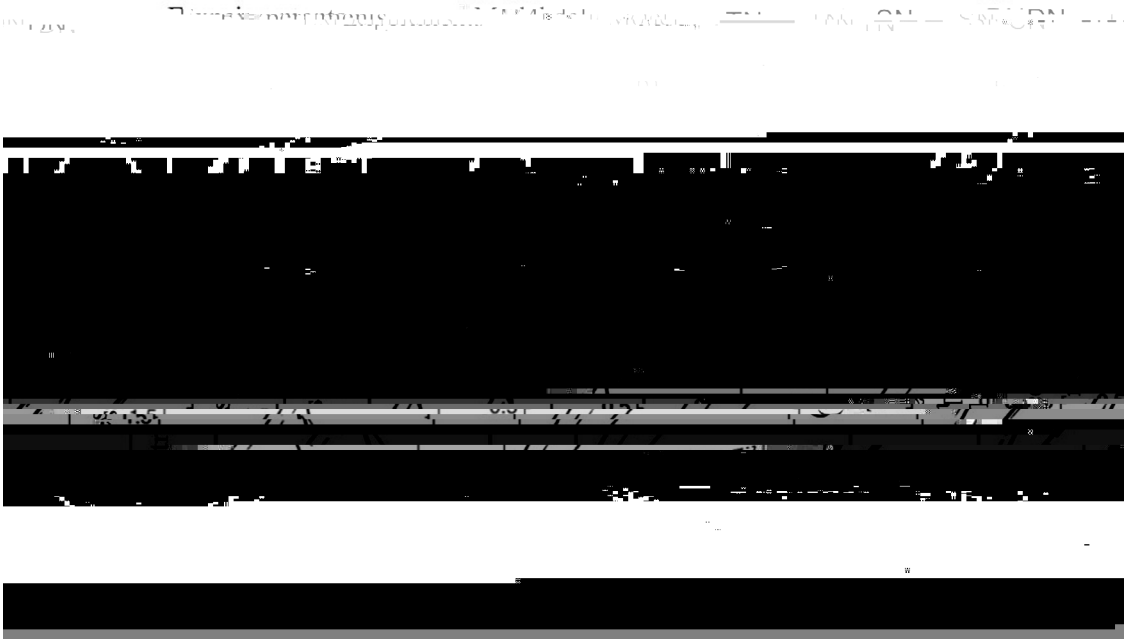

Fig. 5. Cyclic compressive response of rubber under constant loading rate $\dot{\lambda}/k_d = 1/25$. (a) Experimental data from Bergstrom and Boyce (1998) with model comparison. (b) and (c) Predicted time evolution of the chain stretch $\bar{\lambda} = tr(\mu)/3$ and normalized stress $\sigma^i/c^i k_B T$ for the static network SN (dashed lines), dynamic network DN (semi-dashed lined), and their average TN (solid line). (d) Predicted normalized stress-strain response by the kinetic theory. Again, the response is decomposed according to its static SN, dynamic DN, and total TN contributions. Note that the stresses and strains are shown here as positive in compression.

4.2. Cyclic compression of elastomers

In this example, we consider the uniaxial compression of a Chloroprene rubber loaded with carbon black particles as studied in Bergstrom and Boyce (1998). The viscoelastic properties of these elastomers arise from the disruption of entanglements and reptation of long polymer chains during deformation. In other words, an entangled chain may appear as mechanically active at short times, since entanglements may themselves be viewed as physical cross-links. However, as the chain is stretched, over time it will dissociate from the entanglement and evolve towards a more relaxed configuration. This new configuration may also contain entanglements, and this event may therefore be interpreted as an attachment event. Such molecular mechanisms have been captured by the reptation theory of de Gennes (1979), in which the lifetime τ of a physical link was found to scale with the square of chain length. The rate of detachment may therefore be seen as the inverse of this lifetime, i.e., $k_a = k_d = 1/\tau$. We assume here that these rates are independent of time, chain stretch and polymer deformation. Finally, experiments show that this rubber shows a relatively strong

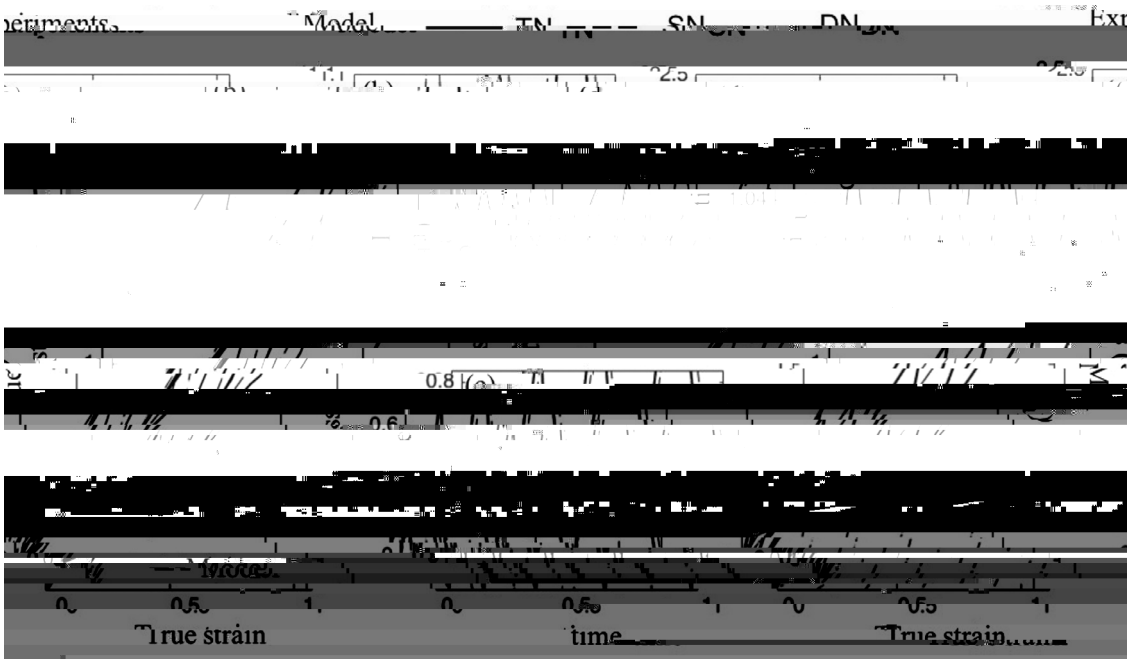

Fig. 6. Repeated cyclic loading under constant loading rate $\dot{\lambda}/k_d = 1/25$ with increasing amplitude. (a) Experimental data from Bergstrom and Boyce (1998) with model comparison. (b) and (c) Predicted time evolution of the chain stretch $\bar{\lambda} = tr(\mu)/3$ and normalized stress $\sigma^i/c^i k_B T$ for the static network SN (dashed

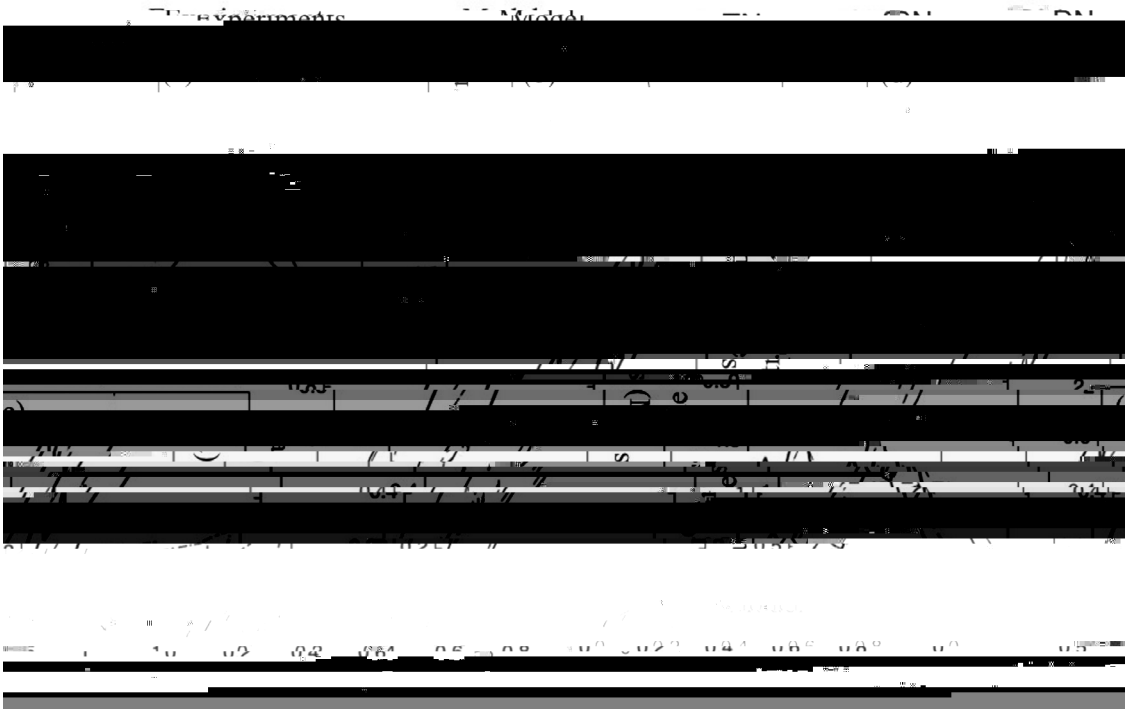

Fig. 7. Cyclic loading with stages of stress relaxation under constant loading rate $\lambda/k_d = 1/25$. (a) Experimental data from Bergstrom and Boyce (1998) with model comparison. (b) and (c) Predicted time evolution of the chain stretch $\bar{\lambda} =$

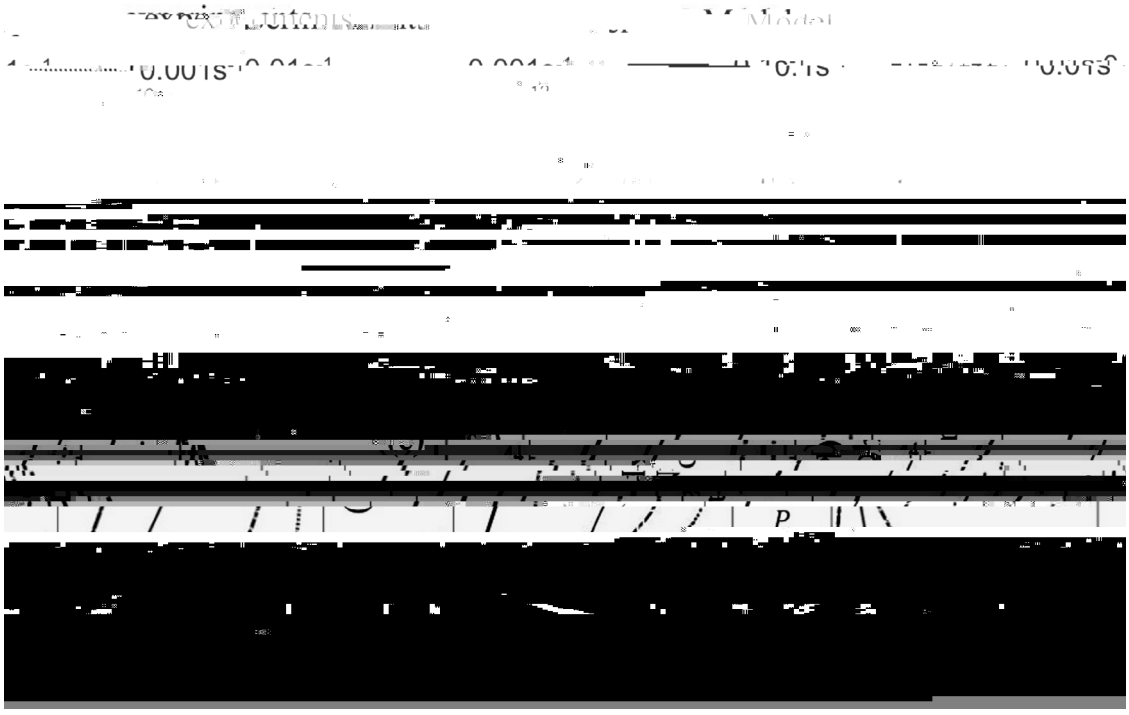

Fig. 8. Cyclic loading of the PVA double network with a loading rate 0.3 s^{-1} and unloading rates 0.1 s^{-1}, 0.01 s^{-1} and 0.001 s^{-1}, respectively. (a) Experimental data from Long et al. (2014). (b) Predicted time evolution of the chain stretch $\bar{\lambda} = tr(\mu)/3$ (thick lines) compared with the average stretch of the sample (thin lines) for unloading rates 0.1 s^{-1} and 0.01 s^{-1}. **(c)** Predicted nominal stress P/ck_BT for unloading rates 0.1 s^{-1} and 0.01 s^{-1}. (d) Predicted stress-strain response by the kinetic theory, to be compared with (a).

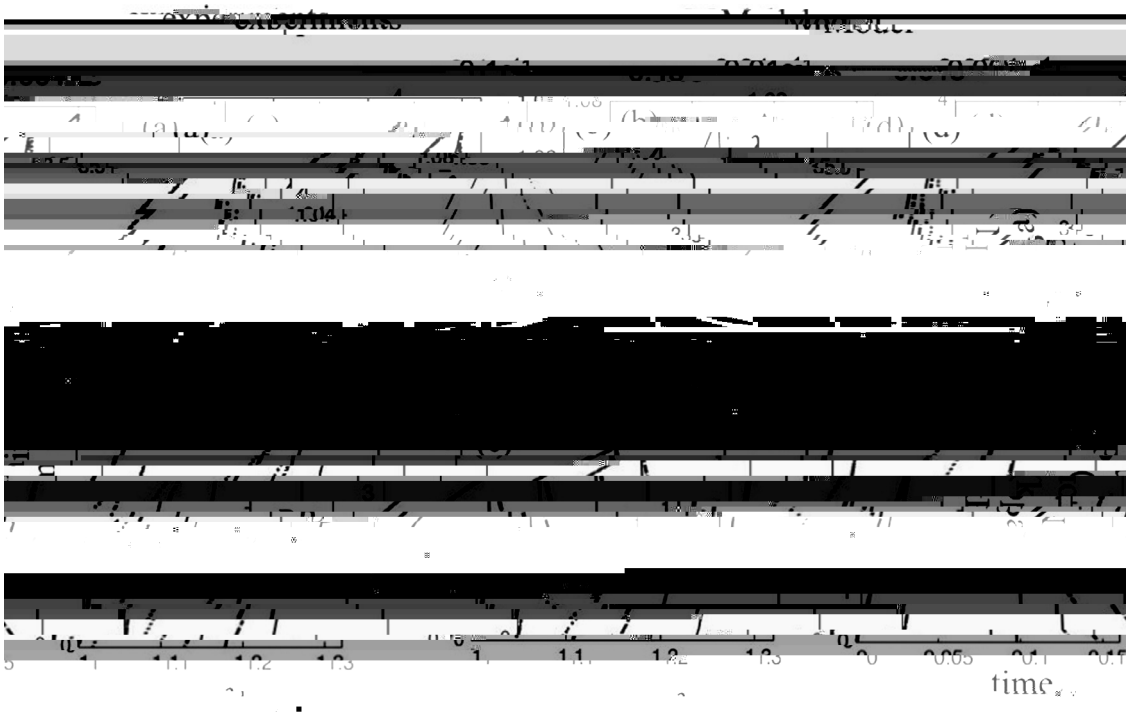

Fig. 9. Cyclic loading of the PVA double network with a loading rate 0.01 s^{-1} and unloading rates 0.1 s^{-1}, 0.01 s^{-1} and 0.001 s^{-1}, respectively. (a) Experimental data from Long et al. (2014). (b) Predicted time evolution of the chain stretch $\bar{\lambda} = tr(\mu)/3$ (thick lines) compared with the average stretch of the sample (thin lines) for unloading0.01 s

we can write:

$$\dot{\psi}(t) = k_a(C-c)\langle\psi\rangle_0 - ck_d\langle\psi\rangle + c\left\langle \frac{1}{\lambda}\frac{d\psi}{d\lambda}\boldsymbol{\lambda}\otimes\boldsymbol{\lambda}\right\rangle : \boldsymbol{L}, \tag{49}$$

$$\dot{\psi}_0(t) = k_a(C-c)\langle\psi\rangle_0 - ck_d\langle\psi\rangle_0 + c\left\langle \frac{1}{\lambda}\frac{d\psi}{d\lambda}\boldsymbol{\lambda}\otimes\boldsymbol{\lambda}\right\rangle_0 : \boldsymbol{L}. \tag{50}$$

Now, applying the mean field approximation, we write:

$$\left\langle \frac{1}{\lambda}\frac{d\psi}{d\lambda}\boldsymbol{\lambda}\otimes\boldsymbol{\lambda}\right\rangle = \frac{1}{\bar{\lambda}}\frac{d\psi}{d\bar{\lambda}}\langle\boldsymbol{\lambda}\otimes\boldsymbol{\lambda}\rangle = \frac{1}{3\bar{\lambda}}\frac{d\psi}{d\bar{\lambda}}\boldsymbol{\mu}, \tag{51}$$

$$\left\langle \frac{1}{\lambda}\frac{d\psi}{d\lambda}\boldsymbol{\lambda}\otimes\boldsymbol{\lambda}\right\rangle_0 = \frac{d\psi}{d\bar{\lambda}}(1)\langle\boldsymbol{\lambda}\otimes\boldsymbol{\lambda}\rangle_0 = \frac{1}{3}\frac{d\psi}{d\bar{\lambda}}(1)\boldsymbol{I}, \tag{52}$$

A discussion regarding the validity of the above approximations is provided in the paragraph following Eq. (22). For this, it is

Long, R., Qi, H., Dunn, M., 2013. Modeling the mechanics of covalently adaptable polymer networks with temperature-dependent bond exchange reactions. Soft Matter 9 (15), 4083–4096. doi:10.1039/C3SM27945F.

Murrell, M., Oakes, P., Lenz, M., Gardel, M., 2015. Forcing cells into shape: the mechanics of actomyosin contractility. Nat. Rev. Mol. Cell Biol. 16 (8), 486–498. doi:10.1038/nrm4012.

Nam, S., Hu, K., Butte, M., Chaudhuri, O., 2016. Strain-enhanced stress relaxation impacts nonlinear elasticity in collagen gels. Proc. Natl. Acad. Sci. U.S.A. 113 (20), 5492–5497. doi:10.1073/pnas.1523906113.

Narita, T., Mayumi, K., Ducouret, G., Hebraud, P., 2013. Viscoelastic properties of poly(vinyl alcohol) hydrogels having permanent and transient cross-links studied by microrheology, classical rheometry, and dynamic light scattering. Macromolecules 46 (10), 4174–4183. doi:10.1021/ma400600f.

Proseus, T., Ortega, J., Boyer, J., 1999. Separating growth from elastic deformation during cell enlargement. Plant Physiol. 119 (2), 775–784.

Purohit, P., Litvinov, R., Brown, A., Discher, D., Weisel, J., 2011. Protein unfolding accounts for the unusual mechanical behavior of fibrin networks. Acta Biomater. 7 (6), 2374–2383. doi:10.1016/j.actbio.2011.02.026.

Rajagopal, K.R., Srinivasa, A.R., 2004. On the thermomechanics of materials that have multiple natural configurations Part i: viscoelasticity and classical plasticity. Zeitschrift für angewandte Mathematik und Physik ZAMP 55 (5), 861–893. doi:10.1007/s00033-004-4019-6.

Rault, J., Marchal, J., Judeinstein, P., Albouy, P., 2006. Stress-induced crystallization and reinforcement in filled natural rubbers: 2h nmr study. Macromolecules 39 (24), 81 Tf .4757 0 TD .1

c [(g r) 1 4 . 6 (o) 1 7 . 7 (w) - . 8 (t h)] T J / F 2 1 T f 3 . 3 2 B r u c c ( ) T h m a